Modeling and Optimization of the Compressive Strength of High Volume Fly Ash ECC with Low Modulus PVA Fiber Using Response Surface Methodology (RSM)

Isyaka Abdulkadir[1,2,a] **& Bashar S. Mohammed**[1,b]

[1] *Civil and Environmental Engineering Department, Universiti Teknologi PETRONAS Malaysia*
[2] *Civil Engineering Department, Bayero University, Kano, Nigeria*

Correspondence : [a]isyaka_18000638@utp.edu.my & [b]bashar.mohammed@utp.edu.my

ABSTRACT

Engineered cementitious composite (ECC) also known as bendable concrete is popular for its high ductility behavior under tensile load. However, to achieve this amazing characteristic, the compressive strength is usually compromised due to the high volume of fly ash (HVFA) effect of reducing the composite's toughness. This research is aimed at developing a response surface model and optimization of the two major ingredients (fly ash and PVA fiber) with the view to developing a composite with the desired compressive strength for structural application. Results indicated that although the FA affects the compressive strength development negatively, the presence of PVA fiber especially at 1 to 1.5% volume fraction enhances the compressive strength. A quadratic response surface model was developed and was analyzed using analysis of variance (ANOVA) and found to have a R^2 value of 96.82%. The model validation showed a very good agreement between the predicted and the experimental results with less than a 5% error margin.

Keywords: ECC, response surface methodology, optimization, high volume fly ash

INTRODUCTION

Since its development in the early 90s, Engineered Cementitious Composite (ECC) has attracted a lot of attention from researchers because of its superior ductility properties (I. Abdulkadir & Mohammed, 2020; H. Ma, 2015; Yu, Lin, Zhang, & Li, 2015). Bendable concrete as it is otherwise called, the ECC came into being as a product of extensive research to find a solution to the inherent weakness of cementitious composites under tensile load. Generally, cementitious composites are excellent in compression but behave poorly under tensile loads. This behavior makes them very prone to cracking. The use of macro-reinforcement in the form of steel bars or micro-reinforcement in the form of randomly incorporated steel fibers has drastically improved the composites' performance under tensile loads. However, fiber-reinforced concrete exhibits tensile softening behavior after the peak load as depicted in Figure 1. With the advent of Ultra-High-Performance Fiber Reinforced Concrete (UHPFRC), the ductility threshold improved tremendously to 0.5%(Abdulkadir & et al., 2020). The ECC as a type of UHPFRC is however the only cementitious composite that shows a pseudo-strain hardening behavior beyond the first crack stress as shown in Figure 1. The materials for making ECC are similar to that of concrete. The only difference is that coarse aggregate is not used to obtain a composite with a low elastic modulus capable of exhibiting the strain hardening behavior that the ECC is known for(Chethan, 2015; Kamal, Khan, Shahzada, & Alam, 2016). The key ingredient used for the attainment of the characteristic ductility and the strain hardening behavior is the polymeric fiber, typically Poly

Vinyl alcohol (PVA) fiber at a very low volume fraction of 2% or less(Zhang, Yuvaraj, Di, & Qian, 2019).

The typical properties of ECC are shown in Table 1. To achieve these properties, micromechanics design principles are adopted to modify the matrix, the fibers, and the matrix-fiber interface. This gives a material with controlled saturated microcracks restricted to a crack width of less than 100μm. As shown in Table 1, ECC has a tensile ductility of $1 - 8\%$ which is 100 to 800 times that of normal concrete (0.01%)(B. S. Mohammed et al., 2020). This is achieved through the fiber bridging mechanism of the PVA fiber leading to the load-bearing capacity beyond the first crack stress (strain hardening).

To get composite with strain hardening behavior entails reducing the toughness, which usually comes at the cost of the mechanical strength of the composite(Li, 2003). Conversely, for an ECC with higher mechanical strength, the tradeoff is usually tensile ductility. Hence, producing an ECC with desirable ductility and strength characteristics requires a careful selection of materials together with sound knowledge of micromechanics design to tailor the fiber, the matrix and their interface for the two basic strain hardening criteria (energy and strength) to be attained as shown in Equations 1 and 2 respectively(Li, 2008).

$$J_{tip} \leq \sigma_0 \delta_0 - \int_0^{\delta_0} \sigma(\delta)\, d\delta \equiv J_b' \tag{1}$$

$$\sigma_0 > \sigma_{CS} \tag{2}$$

Where; J_{tip} is the crack tip toughness; σ_0 is maximum fiber bridging stress; δ_0 is the crack width corresponding to σ_0; J_b' is the complementary energy; σ_{CS} is the cracking strength of the matrix.
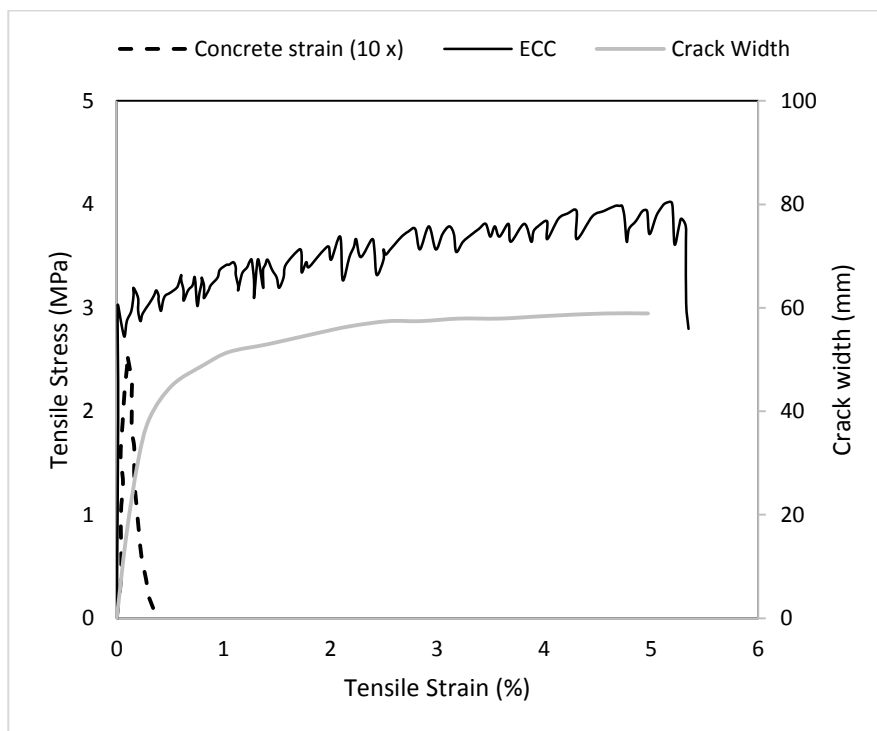
Figure 1. Typical tensile stress-strain curve for ECC(Abdulkadir & et al., 2020)

Table 1. Properties of ECC

Compressive Strength (MPa)	First Crack Strength (MPa)	Ultimate Tensile Strength (MPa)	Ultimate Tensile Strain (%)	Young's Modulus (GPa)	Flexural Strength (MPa)	Density (g/cc)
20-95	3-7	4-12	1-8	18-34	10-30	0.95-2.3

Tailoring the ECC entails adjusting the materials to satisfy the strength and energy criteria. The matrix fracture toughness can be reduced by adjusting the water-cement ratio, the aggregate type, and the cement/fly ash content of the mix. This will limit the amount of J_{tip} and consequently lower the matrix first crack strength. Similarly, by adjusting the fiber properties such as the length, volume, and aspect ratio, the energy criterion can be satisfied(Yun Yong Kim, 2003). This ensures that the first crack strength does not exceed the fiber bridging stress so that the saturated multiple microcracks responsible for the strain hardening behavior can be developed. Otherwise, strain-softening behavior similar to FRC occurs due to the development of big cracks (Griffith crack). These requirements make the use of optimization in ECC very essential.

RSM is a design of experiment (DoE) method in which mathematical and statistical techniques are used for the determination of the relationship between input parameters known as the independent variables and the dependent variable called the response (V. C. Khed, Mohammed, Liew, & Abdullah Zawawi, 2020; Lye, Mohammed, Liew, Wahab, & Al-Fakih, 2020; Bashar S. Mohammed, 2018). Furthermore, the RSM is used in developing mathematical models for predicting the response at different levels of the variables. The normal procedure involves firstly designing a series of experiments to obtain experimental data for the response(s) of interest. Secondly, using the experimental data, numerical models of the responses are developed and validated by analyses of variance (ANOVA). The final stage is optimizing the input variables intending to obtain a defined level of the response variable(Ghafari, Costa, & Júlio, 2014).

A lot of research works on the use of RSM exist. Mohammed *et al.* (Bashar S. Mohammed, Haruna, Mubarak bn Abdul Wahab, & Liew, 2019) used RSM to characterize cast-in-situ alkali-activated sludge. Khed et al developed RSM models for the bond behavior of self-compacting hybrid fiber reinforced rubberized cementitious composite. Similarly, Abdulkadir and Mohammed (I. Abdulkadir & Mohammed, 2020) used RSM for the study on the six months compressive strength development and shrinkage behavior of high volume fly ash rubberized ECC. RMS-based models for the prediction of the performance of self-compacting UHPC reinforced with hybrid steel microfibers were developed by Ghafari *et al.* (Ghafari et al., 2014). Many similar works on the development of RSM-based models for the properties of concrete(Bashar S. Mohammed, Fang, Anwar Hossain, & Lachemi, 2012; Rezaifar, Hasanzadeh, & Gholhaki, 2016), roller compacted concrete(Adamu, Mohammed, Shafiq, Liew, & Alaloul, 2018; Adamu, Mohammed, & Shahir Liew, 2018) and different forms of ECC (V. C. Khed, Mohammed, & Nuruddin, 2018; V. C. M. Khed, Bashar S. Mohd; Shahir Liew; Alaloul, Wesam S.; Musa Adamu, Amin Al-Fakih, 2018; Bashar S. Mohammed, Achara, Liew, Alaloul, & Khed, 2019) have been carried out.

Due to the need for ECC to exhibit good tensile ductility, most researchers focus on the tailoring of the ingredients towards achieving that. Usually, the tensile strain capacity is achieved at the cost of other mechanical strengths (compressive strength, flexural strength, and tensile strength. However, the importance of compressive strength should not be compromised at all costs. This is because of the increasing popularity as a repair material and a choice material for the construction of link slabs and coupling beams. In all these situations, the strength of the material is as important as the ductility and deformation characteristics.

This research aims to develop a compressive strength model and perform optimization to determine the best combination of the HVFA and PVA fiber that will yield the optimum compressive strength. This will be done using the RSM approach.

METHODOLOGY

Materials

First, Ordinary Portland cement Type-1 conforming to the requirements of ASTM C150 named Castle from YTL cement company Malaysia was used. The chemical composition and physical properties of the OPC and Fly ash are presented in Table 2. The Fly ash used conforms to the specifications of ASTM C168-10 classified as class F for having a total Al_2O_3, SiO_2, and Fe_2O_3 of more than 70% as shown in Table 2. River sand has a specific gravity of 2.65 and a maximum particle size of 1.18 mm as shown in the grading curve in Figure 2. The PVA fiber used is from Kuraray Company Japan having an oil coating of 1.2% by weight. The surface oil coating is to reduce the development of an excessive chemical bond between the fiber and the cement paste which could lead to fiber rupture under load. The properties of the PVA fiber are presented in Table 3. To ensure adequate flowability as a self-compacting mix, "Sika ViscoCrete-2044" a poly carboxylate-based high-range water-reducing (HRWR) admixture was used.

RSM design

In this research, the composite was tailored to achieve the desired result by setting the PVA fiber volume fraction and the FA percentage replacement of cement as the variables (input parameters), while maintaining the fine aggregate content and water-cement ratio constant based on the number of materials required for the standard ECC-M45. The range of the PVA and FA were set at 1 − 2 % and 50 − 70 % as the low and high levels respectively. Using the Design-Expert software (version 10), the Central Composite Design option of the RSM was adopted and 13 mixes were developed as shown in Table 4.

Table 2. Properties of PVA Fiber

Length (mm)	Diameter (μm)	Aspect Ratio	Density (g/cm3)	Tensile Strength (MPa)	Modulus of Elasticity (GPa)
18	200	90	1.3	750	7.1

Table 3. Chemical composition of OPC and FA

Chemical Oxide	OPC (%)	FA (%)
SiO2	20.76	57.01
Al2O3	5.54	20.96
Fe2O3	3.35	4.15
MnO	-	0.033
CaO	61.4	9.79
MgO	2.48	1.75
Na2O	0.19	2.23
K2O	0.78	1.53
TiO2	-	0.68
LOI	2.2	1.25
Specific gravity	3.15	2.38
Blaine fineness (m2/Kg)	325	290

Table 4. Mix Proportion of HVFA-ECC per m^3

Mix	PVA (%)	FA (%)	PVA kg/m^3	FA kg/m^3	Cem. kg/m^3	Fine Agg. kg/m^3	Wat. kg/m^3
M11	1.5	60	19.5	770	513	467	320
M12	1.5	60	19.5	770	513	467	320
M8	1.5	70	19.5	898	385	467	320
M6	2	60	26.0	770	513	467	320
M7	1.5	50	19.5	642	642	467	320
M9	1.5	60	19.5	770	513	467	320
M4	2	70	26.0	898	385	467	320
M5	1	60	13.0	770	513	467	320
M3	1	70	13.0	898	385	467	320
M10	1.5	60	19.5	770	513	467	320
M1	1	50	13.0	642	642	467	320
M2	2	50	26.0	642	642	467	320
M13	1.5	60	19.5	770	642	467	320
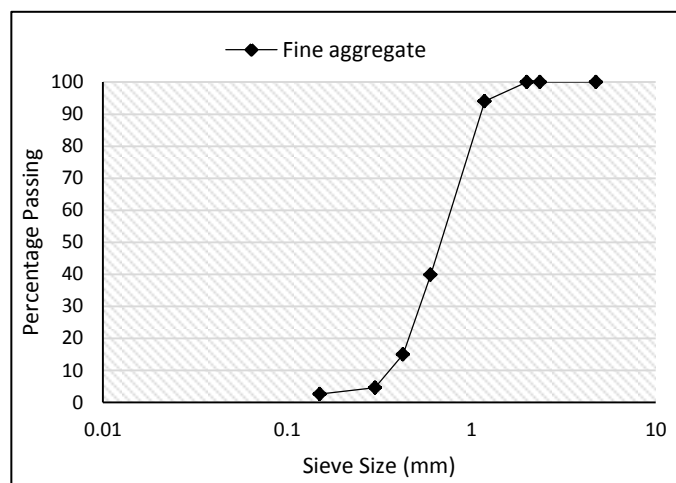
Figure 2. Grading curve for fine aggregate

Mixing, Casting, and Testing Procedure

All the dry materials including the cement, FA, and Fine aggregate except the PVA were first dry-mixed for 2 minutes in a Pan-type concrete mixer with double rotation. Next, the water and the HRWR were added to the dry materials and further mixed for 3 minutes. Lastly, the PVA fiber was gradually added to the mix by sprinkling while mixing to ensure adequate dispersion and prevent fiber clumping. The mixing was continued for 5 more minutes to ensure that all the fiber was properly dispersed within the mix and no cluster was visible as shown in Figure 3 (a). After mixing, the samples were cast in molds (Figure 3 (b)) and left to sit for 24 hours before demolding as shown in Figure 3 (c), and then cured in a water tank for 28 days at 20°C and 95% relative humidity.
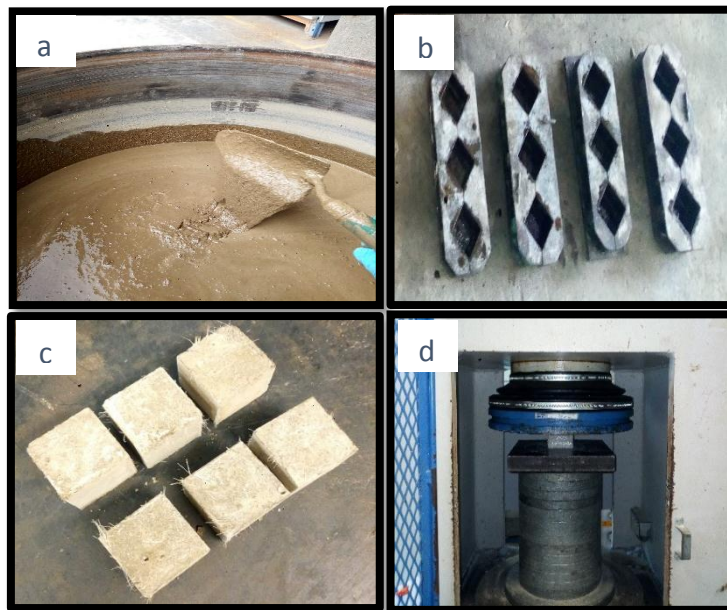
Figure 3. *(a)* Fresh HVFA-ECC Mix (b) Oiled 50 mm molds (c) Cast samples after 24 hours (d) Compressive strength test

As shown in Figure 3 (d), the compressive strength of the HVFA-ECC for all the 13 different mixes was determined using 50 mm cube samples subjected to a gradually increasing axial compressive load via a 3000 kN Universal Testing Machine (UTM) fitted with an electronic digital screen display. The test was conducted based on the provisions of BS EN 12390-3. Three cube samples were tested at the end of the 28 days curing duration and the average of the three readings was recorded as the compressive strength.

RESULTS AND DISCUSSIONS

Table 5 presents the responses obtained at 28 days of curing after experimental tests carried out on all mixes at 28 days of curing. The influence of the variables (FA and PVA) and their interactions on the responses (compressive strength, flexural strength, and tensile strain capacity) were investigated and analyzed.

Composite Compressive Strength

The compressive strength of the composite generally increased with an increase in the curing duration for all the 13 mixes as shown in Figure 4. The rate of the strength gain of the composite is similar across the whole mixes. The figure shows the values of the compressive of the HVFA-ECC at 28 days of curing for all the mixes. The result indicated a decrease in

strength with an increase in the amount of cement replacement with FA. The mixes having the highest amount of FA replacement (70%) exhibited the lowest strength at 28 days for all PVA fiber content followed by those having 60% FA. The lower strength values exhibited by the mixes having higher FA content are attributed to two factors. The first is that the reaction of FA with the cement hydration products (secondary hydration) is usually slow in the early days of the composite up to 28 days because the cement has not fully hydrated. The strength is expected to increase after 28 days when the secondary hydration yields more calcium silica hydrate (C-S-H). Secondly, due to the low water-cement ratio of the mix (0.25), most of the FA remains unreacted and serves just as a filler within the matrix.

Table 5. Compressive strength at 28 days (Response)

MIX Number	Variables		Response
	PVA (%)	Fly Ash (%)	Compressive Strength (MPa)
M11	1.5	60	52.96
M12	1.5	60	51.19
M8	1.5	70	47.66
M6	2	60	50.82
M7	1.5	50	56.25
M9	1.5	60	53.03
M4	2	70	45.15
M5	1	60	48.85
M3	1	70	46.79
M10	1.5	60	52.55
M1	1	50	50.09
M2	2	50	54.87
M13	1.5	60	52.91
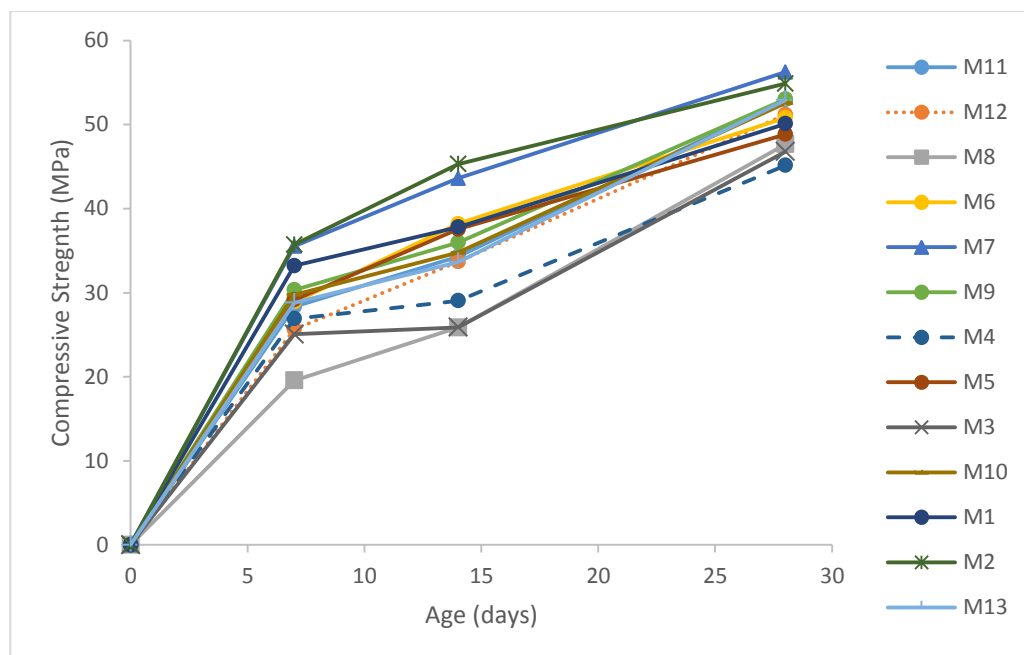
Figure 4. Compressive strength development of low modulus PVA fiber HVFA-ECC

In the same vein, the presence of PVA fiber seems to contribute to the compressive strength of the composite, especially at percentages of 1 and 1.5. This can be observed from the result of mixes having the same FA replacement levels but different PVA content. For Example, M5 has a compressive strength of 48.85 MPa which is lower than the compressive strength of all other mixes having the same FA replacement (60%) but different PVA content (M6, M10, M11, and M12). However, the highest level of the PVA (2%) affects the compressive strength negatively. Consistently, 2% PVA addition led to a lower compressive strength than 1.5% PVA for all the mixes having similar FA composition. This behavior was observed by other researchers and it is caused by the tendency of the PVA fiber to clump together during mixing and therefore creating patches within the matrix that has adequate cement paste to bond the clumped fibers.

Figures 4 and 5 respectively show the 2D contour and 3D response surface plots depicting the effect of the variables (PVA and FA) on the compressive strength and also how the interaction between the variables affects the response (compressive strength). The figures show what was discussed earlier on the negative effect of FA on the compressive strength of the ECC. The red zone depicts an area of higher compressive strength which lies around the FA replacement levels of 50 to 55%. Similarly, the amount of PVA fiber corresponding to the highest compressive strength values (54 to 56 MPa) is between 1.3% and 2%. As for the interaction between the two variables, the range between 50 to 55% FA replacement of cement and 1.3 to 2% of PV addition yield the highest value of compressive strength (54 to 54 MPa). As one moves away from this range of values of the variables, the compressive strength of the composite is negatively affected.
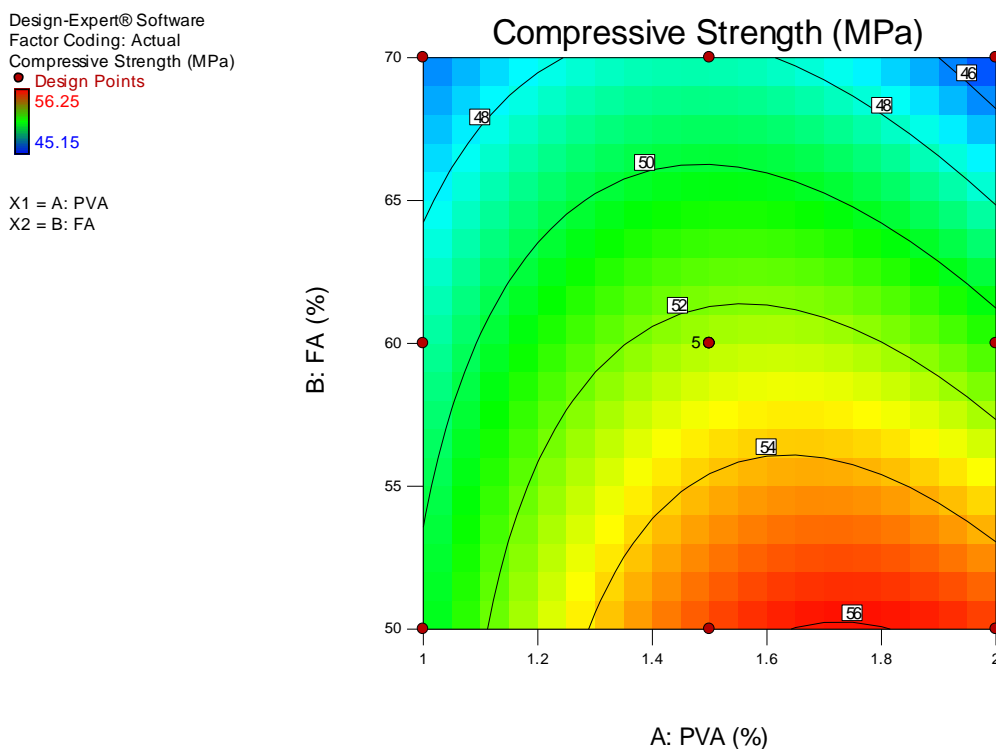
Figure 4. 2D response surface plot for compressive strength at 28 days
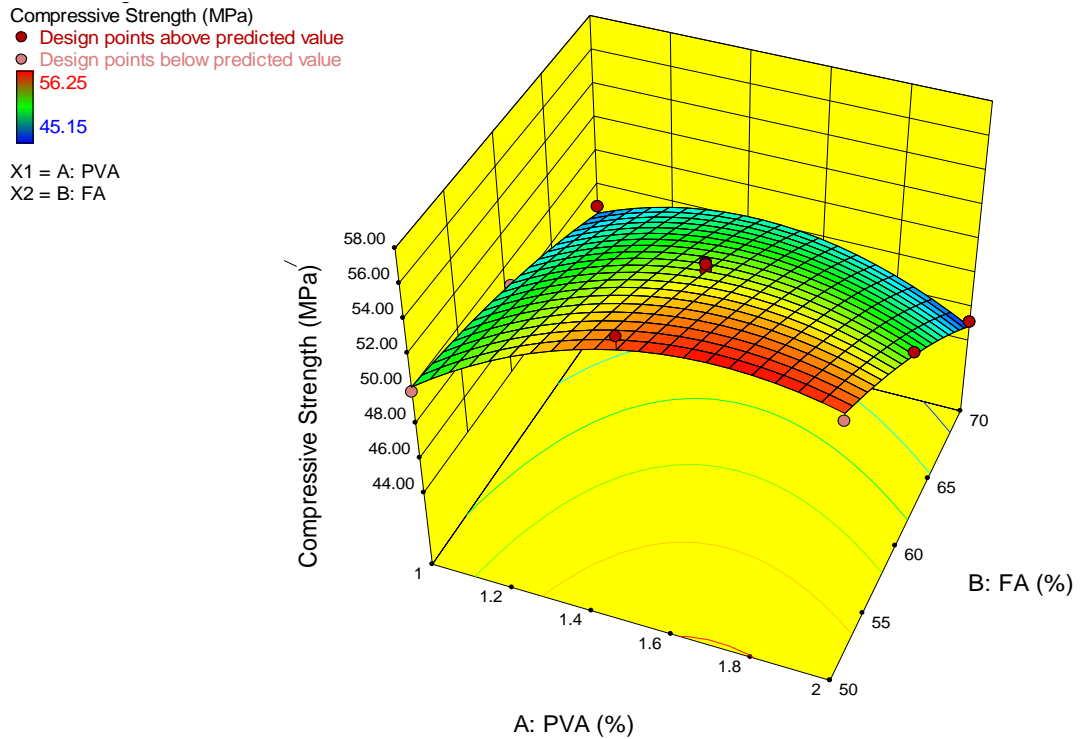
Figure 5. 3D response surface diagram for compressive strength

Response Surface Model and ANOVA

The aim of using the RSM is to develop a response surface model for the response and to be able to carry out an analysis of variance for the response. For this particular response (compressive strength) quadratic function proved most appropriate as the model. Using the ANOVA, the model was validated accordingly. Table 6 presents the summary of the ANOVA.

Table 6. ANOVA summary

Response	Source	Sum of Squares	Df	Mean Square	F - Value	P-Value > F	Significance
Compressive	Model	120.31	5	24.06	42.63	0.00004	YES
Strength	A – PVA	4.35	1	4.35	7.71	0.02652	NO
	B – FA	77.83	1	77.83	137.91	0.00001	YES
	AB	10.30	1	10.30	18.26	0.00353	YES
	A^2	19.79	1	19.79	35.06	0.00052	YES
	B^2	0.86	1	0.86	1.52	0.2579	NO

The response surface model developed (in coded factors) for the interaction of the variables on the response is shown in equations (3). The RSM by default assigns a value of +1 for the highest levels of the variables and -1 for the lowest while 0 is assigned for the intermediate levels as the codes. The model equation in terms of the actual factors is shown in Equation 4. The analysis was done based on a 95% percent confidence interval (i.e. 5% level of significance). Therefore, it can be seen that for compressive strength, A, B, AB, and A^2 are significant model terms. For the model to fit, the *Lack of fit P-value* has to be more than the 5% level of significance. Hence the lack of fit value of 0.82, was not significant relative to the pure error. This means that the chance of a lack of fit F-value this large occurring due to noise is 54.73. This is a good indication that the model will fit.

The R^2 values of the response are another indicator of the quality of the model. The higher the R^2-value, the better the model. Table 7 gives the model validation values for the response. The R^2 value for the response is 97%. Similarly, the difference between the *Predicted R^2* and the Adjusted R^2 should be less than 0.2 for the model to fit. In this case, the value of the *Predicted R^2* is in reasonable agreement with the *Adjusted R^2* for having a difference of less than 0.2. Another indicator of model quality is the *Adequate Precision* value. This value measures the signal-to-noise ratio and a value of more than 4 is desirable. The adequate precision value for the response is 20.834 and this indicates that the model can be used to traverse the design space adequately.

$$\text{Comp. Strength} = 52.53 + 0.85A - 3.60B - 1.61AB - 2.71A^2 - 0.59B^2 \qquad (3)$$

$$\text{Comp. Strength} = -2.97 + 53.49 * PVA + 0.83 * FA - 0.32 * PVA * FA - 10.84 * PVA^2 - 5.91 * FA^2 \qquad (4)$$

Table 7. ANOVA validation

Model Validation Parameters	Response
	Compressive Strength (MPa)
Std. Dev.	0.75
Mean	50.98
C.V. %	1.47
PRESS	18.85
-2Log Likelihood	21.41
R^2	0.9682
Adj. R^2	0.9455
Pred. R^2	0.8483
Adeq. Precision	20.834
BIC	36.80
AIC	47.41

The response surface model can also be validated by the normality plot as shown in Figure 8. The normal plot of the residuals for compressive strength indicated a good fit due to the linearity of the point along the straight line as depicted in the figure. The more linear the points are, the more accurate is the model. Similarly, using the plot of the predicted and the actual result as shown in Figure 9, the accuracy of the model can be assessed under how the results agree with each other with points following a linear pattern. Therefore, by all measures, the model developed can be used for the determination of compressive strength at 28 days at different levels of PVA fiber volume fractions and FA replacement of cement with a high degree of accuracy.
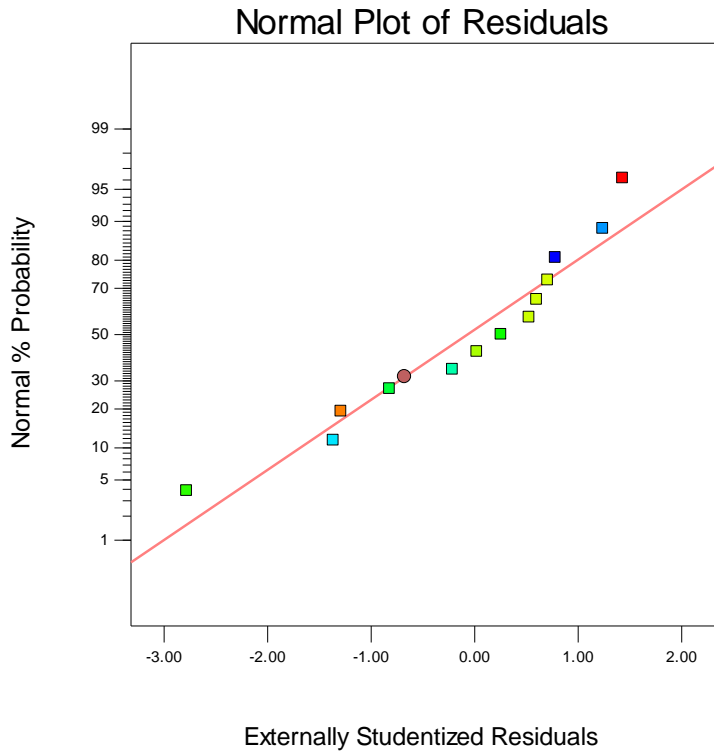
Figure 8. Normality plot for 28 days compressive strength
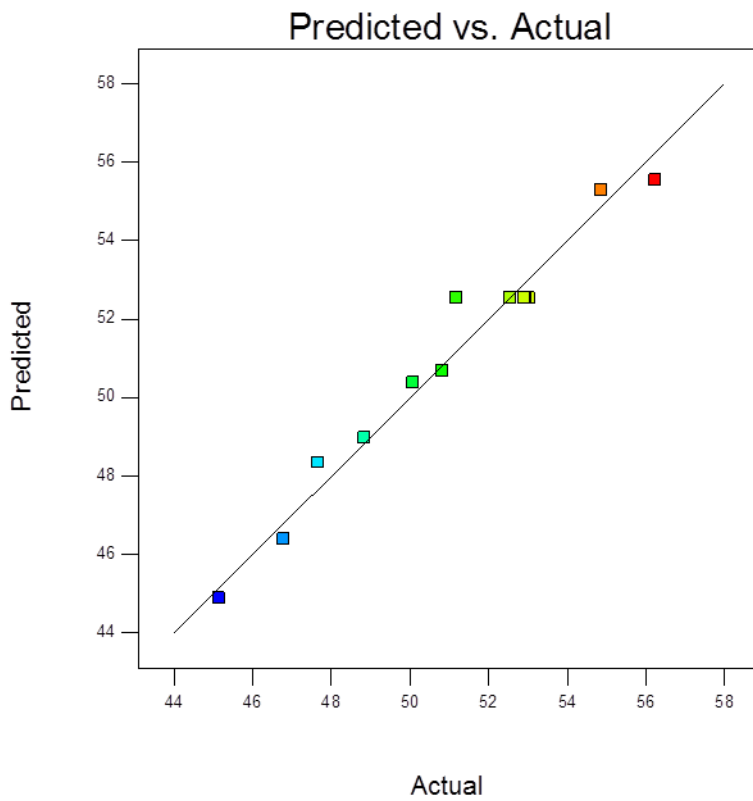
Figure 9. Plot of predicted versus the actual result for the 28-day compressive strength

Optimization

After the numerical model was developed and validated, optimization was carried out. The optimization aimed to get the best levels of the variables that will lead to the most desirable response. The optimization result is assessed by a desirability value on a scale of 0 to 1 (0 to 100%). This is achieved by selecting a goal for the variables (maximum, minimum or in range) and the response (maximize or minimize) and allowing the RSM to operate. A value of desirability close to one indicates the high accuracy and relevance of the response model.

The optimization was performed with the goals set as shown in Table 8. The result of the optimization is shown in Table 8 and Figure 10 respectively. The desirability of 83.33% was obtained and that shows how good the result of the optimization is. For the experimental validation of the model, a new mix using the optimum values of the variables was produced in the laboratory and tested at the end of 28 days of curing. Three samples were produced and the average of the reading is taken as the compressive strength. The result is shown in Table 9. It turned out that there is a high correlation between the predicted and the experimental with a percentage error of less than 5% (the acceptable limit). Hence this indicates that the response models can be used to predict the responses with high accuracy.

Table 8. Optimization goals and results

		Variable		Response
		PVA (%)	FA (%)	Compressive Strength (MPa)
Value	Minimum	1	50	45.15
	Maximum	2	70	56.25
Goal		In range	In range	Maximize
Optimization result		1.73	50	56.08
Desirability		98.5%		

Table 9. Experimental validation

Response	Predicted	Experimental	Error (%)
Compressive Strength (MPa)	56.08	55.22	3.09

A:PVA = 1.72927

B:FA = 50

Compressive Strength = 56.0848

Desirability = 0.985
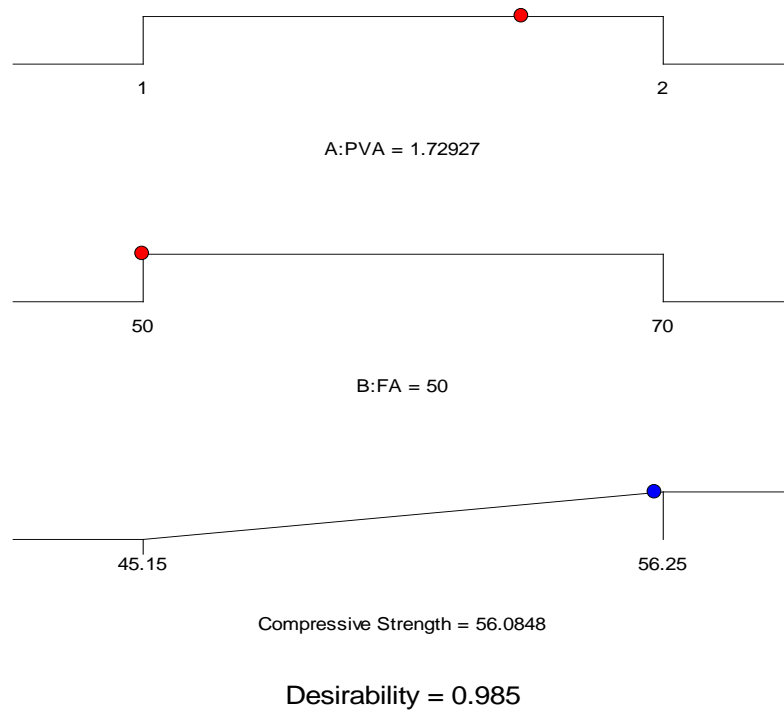
Figure 10. Optimization Rampm diagram

CONCLUSION

This research was conducted to model the compressive strength of HVFA-ECC with low modulus PVA fiber and perform optimization using RSM. At the end of the research, the following conclusions were drawn :

1. The use of HVFA negatively affects the compressive strength of the ECC.
2. The presence of PVA fiber enhances the compressive strength of the composite as mixes having the same amount of FA but different PVA content showed an enhanced strength with 1% and 1.5% PVA. Although the strength is sometimes negatively affected by the high volume fraction of the PVA fiber (2%).
3. The response surface model was successfully developed and validated using ANOVA.
4. Optimization was performed and verified with the predicted and experimental results having a high level of agreement with a margin of error of less than 5%.

It is recommended that to achieve a HVFA-ECC with over 50 MPa compressive strength, PVA fiber of 1.73% volume fraction should be used at 50% cement replacement with FA.

REFERENCES

Abdulkadir, & et al. (2020). "A review of the effect of waste tire rubber on the properties of ECC". *International Journal of ADVANCED AND APPLIED SCIENCES, 7*(8), 105-116. doi:10.21833/ijaas.2020.08.011

Abdulkadir, I., & Mohammed, B. S. (2020). "RSM Study and Analysis on the 6 months Compressive Strength Development and Shrinkage Behavior of High Volume Fly Ash ECC (HVFA-ECC)". *International Journal of Advanced Research in Engineering and Technology (IJARET), 11*(9), 965-980.

Adamu, M., Mohammed, B. S., Shafiq, N., Liew, M. S., & Alaloul, W. S. (2018). "Effect of crumb rubber and nano-silica on the durability performance of high volume fly ash roller compacted concrete pavement". *International Journal of ADVANCED AND APPLIED SCIENCES, 5*(10), 53-61. doi:10.21833/ijaas.2018.10.008

Adamu, M., Mohammed, B. S., & Shahir Liew, M. (2018). "Mechanical properties and performance of high volume fly ash roller compacted concrete containing crumb rubber and nano-silica". *Construction and Building Materials, 171*, 521-538. doi:https://doi.org/10.1016/j.conbuildmat.2018.03.138

Chethan, V. R., Dr. M. Ramegowda, Manohara. H.E. (2015). "ENGINEERED CEMENTITIOUS COMPOSITES-A REVIEW". *International Research Journal of Engineering and Technology (IRJET), 2*(5), 144-149.

Ghafari, E., Costa, H., & Júlio, E. (2014). "RSM-based model to predict the performance of self-compacting UHPC reinforced with hybrid steel micro-fibers". *Construction and Building Materials, 66*, 375-383. doi:10.1016/j.conbuildmat.2014.05.064

H. Ma, S. Q., V. C. Li. (2015). "Development of Engineered Cementitious Composite with local material ingredients*". Paper presented at the High-Performance Fiber Reinforced Cement Composites*, Stuttgart, Germany.

Kamal, M., Khan, S. W., Shahzada, K., & Alam, M. (2016). "Experimental investigation of the mechanical properties of Engineered Cementitious Composites (ECC)". *International Journal of Advanced Structures and Geotechnical Engineering, Vol. 05*(No. 02), 2319-5347.

Khed, V. C., Mohammed, B. S., Liew, M. S., & Abdullah Zawawi, N. A. W. (2020). "Development of response surface models for self-compacting hybrid fiber reinforced rubberized cementitious composite". *Construction and Building Materials, 232*, 117191. doi:https://doi.org/10.1016/j.conbuildmat.2019.117191

Khed, V. C., Mohammed, B. S., & Nuruddin, M. F. (2018). "Effects of different crumb rubber sizes on the flowability and compressive strength of hybrid fiber reinforced ECC". *IOP Conference Series: Earth and Environmental Science, 140*. doi:10.1088/1755-1315/140/1/012137

Khed, V. C. M., Bashar S. Mohd; Shahir Liew; Alaloul, Wesam S.; Musa Adamu, Amin Al-Fakih. (2018). "Experimental Investigation on Pullout Strength of Hybrid Reinforcement of Fibre in Rubberized Cementitious Composites". *International Journal of Civil Engineering and Technology (IJCIET), 9*(7), 1612–1622.

Li, V. C. (2003). "On Engineered Cementitious Composite: A review of the Material and its applications". *Journal of Advanced Concrete Technology, 1*(3).

Li, V. C. (2008). "Engineered Cementitious Composites (ECC) – Material, Structural, and Durability Performance". In E. Nawy (Ed.), *Concrete Construction Engineering Handbook*: CRC Press.

Lye, H. L., Mohammed, B. S., Liew, M. S., Wahab, M. M. A., & Al-Fakih, A. (2020). "Bond-behavior of CFRP-strengthened ECC using Response Surface Methodology (RSM)". *Case Studies in Construction Materials, 12*. doi:10.1016/j.cscm.2019.e00327

Mohammed, B. S. (2018). "Evaluating the Static and Dynamic Modulus of Elasticity of Roller Compacted Rubbercrete Using Response Surface Methodology". *International Journal of GEOMATE, 14*(41). doi:10.21660/2018.41.42833

Mohammed, B. S., Achara, B. E., Liew, M. S., Alaloul, W. S., & Khed, V. C. (2019). "Effects of elevated temperature on the tensile properties of NS-modified self-consolidating engineered cementitious composites and property optimization using response surface methodology (RSM)". *Construction and Building Materials, 206*, 449-469. doi:10.1016/j.conbuildmat.2019.02.033

Mohammed, B. S., Fang, O. C., Anwar Hossain, K. M., & Lachemi, M. (2012). "Mix proportioning of concrete containing paper mill residuals using response surface methodology". *Construction and Building Materials, 35*, 63-68. doi:10.1016/j.conbuildmat.2012.02.050

Mohammed, B. S., Haruna, S., Mubarak bn Abdul Wahab, M., & Liew, M. S. (2019). "Optimization and characterization of cast-in-situ alkali-activated pastes by response surface methodology". *Construction and Building Materials, 225*, 776-787. doi:10.1016/j.conbuildmat.2019.07.267

Mohammed, B. S., Yen, L. Y., Haruna, S., Seng Huat, M. L., Abdulkadir, I., Al-Fakih, A., . . . Abdullah Zawawi, N. A. W. (2020). "Effect of Elevated Temperature on the Compressive Strength and Durability Properties of Crumb Rubber Engineered Cementitious Composite". *Materials (Basel), 13*(16). doi:10.3390/ma13163516

Rezaifar, O., Hasanzadeh, M., & Gholhaki, M. (2016). "Concrete made with hybrid blends of crumb rubber and metakaolin: Optimization using Response Surface Method". *Construction and Building Materials, 123*, 59-68. doi:10.1016/j.conbuildmat.2016.06.047

Yu, J., Lin, J., Zhang, Z., & Li, V. C. (2015). "Mechanical performance of ECC with high-volume fly ash after sub-elevated temperatures". *Construction and Building Materials, 99*, 82-89. doi:10.1016/j.conbuildmat.2015.09.002

Yun Yong Kim, H.-J. K., and Victor C. Li. (2003). "Design of Engineered Cementitious Composite Suitable for Wet-Mixture Shotcreting". *ACI Materials Journal, 100*(02).

Zhang, Z., Yuvaraj, A., Di, J., & Qian, S. (2019). "Matrix design of lightweight, high strength, high ductility ECC". *Construction and Building Materials, 210*, 188-197. doi:10.1016/j.conbuildmat.2019.03.159